Heliyon 9 (2023) e22352

Contents lists available at ScienceDirect

Heliyon

journal homepage: www.cell.com/heliyon

Layered energy-saving speed planning and control method for electric vehicle on continuous signal lights road

Jing Jiao [a], Liguo Zang [a,b,*], Yulin Mao [a], Cheng Xue [a], Xinlei Peng [a]

[a] School of Automobile and Rail Transportation, Nanjing Institute of Technology, Nanjing, 211167, China
[b] State Key Laboratory of Automotive Simulation and Control, Changchun, 130015, China

ARTICLE INFO

Keywords:
Energy consumption
Electric vehicle
Model predictive control
Ride comfort
Sinusoidal variable speed curve
Vehicle speed planning and control

ABSTRACT

Emergency start-stop in front of signal lights is one of the main reasons for additional energy consumption and ride discomfort of Electric Vehicle (EV). Existing research on this issue rarely takes into account both energy consumption and ride comfort. Therefore, the layered energy-saving speed planning and control method is proposed. The upper is the layer of energy-saving speed planning. This layer reduces energy consumption of EV by reducing the number of stops on continuous signal lights road and minimizing the range of speed change. On this basis, the sinusoidal variable speed curve is used to smooth the acceleration process to improve ride comfort. Finally, the energy-saving speed considering ride comfort is obtained. This layer makes up for the issue that existing research rarely takes into account both energy consumption and ride comfort of EV, and is an extension and innovation of existing research. The lower is the layer of Model Predictive Controller (MPC)-based speed control. Based on the longitudinal dynamics model of EV, the MPC-based speed controller is established to control EV to track the energy-saving speed. The controller is easy to understand and implement, and it is also suitable for other research on EV, which has certain application value. The simulation results show that under various working conditions, the maximum energy consumption of EV passing through continuous signal lights road without stopping is 604.29 kJ/km, and the minimum is 244.76 kJ/km. The energy consumption is lower than that of actual road test, and it can be saved by 23.18 % compared with the method in the same field. The maximum Root Mean Square of accelerations (RMS_a) is 0.25 m/s^2, and the minimum is 0.10 m/s^2. The values of RMS_a above are lower than 0.315 m/s^2, which indicates that the ride comfort is good. The utilized method can reduce energy consumption of EV, improve its range and ride comfort, which has important reference significance for promoting the development of EV.

1. Introduction

The development of Electric Vehicle (EV) reduces the dependence of vehicles on fossil fuels. However, due to the limitation of battery capacity and energy density, the mileage of EV is relatively short. Therefore, reducing energy consumption and increasing mileage are the problems that must be solved for the further development of EV [1,2]. Continuous signal lights road is important driving scene in urban traffic. Emergency start-stop in front of signal lights will not only increase the energy consumption, but also

* Corresponding author. School of Automobile and Rail Transportation, Nanjing Institute of Technology, Nanjing, 211167, China
E-mail addresses: 2806914582@qq.com (J. Jiao), zangliguo@njit.edu.cn (L. Zang), 2568806435@qq.com (Y. Mao), y00450220226@njit.edu.cn (C. Xue), 2287804998@qq.com (X. Peng).

https://doi.org/10.1016/j.heliyon.2023.e22352
Received 23 July 2023; Received in revised form 28 October 2023; Accepted 9 November 2023
Available online 17 November 2023

reduce the ride comfort. The method of speed planning and control is an important solution to reduce the emergency start-stop of EV, thereby reducing energy consumption and improving ride comfort [3–5].

In recent years, scholars at home and abroad have conducted in-depth research on energy-saving speed planning and control. Han et al. [6] utilized the Dijkstra algorithm to search for the optimal time and speed for vehicles entering signal light sections. The method establishes an energy-optimal speed trajectory for vehicles, enabling them to pass signal light intersections in an energy-saving manner. Chen et al. [7] established an optimal speed planning model, considering constraints such as traffic lights and speed. The energy-saving problem at signal light road is transformed into the segmented optimal speed planning problem. Similarly, Zhuang et al. [8] also adopted this method to solve the energy-saving problem of EV in front of signal lights. Wu et al. [9] proposed a method that jointly plans speed and signal light timing. While planning speed based on signal light information, the method dynamically adjusts the starting time and duration of green light phases using a sliding time window approach. Compared to pure speed planning approaches, this method reduces both energy consumption and travel delay.

The aforementioned speed planning methods assume that vehicles are operating in a free-flowing traffic environment, which do not consider the influence of preceding vehicles on their own speed. Furthermore, Nie et al. [10] proposed a real-time dynamic predictive cruising control system that integrates the constraints of preceding vehicles and signal lights. At each sampling step, this system computes an expected acceleration command as the optimal control signal. This allows vehicles to pass through the nearest signal light intersection during the green light duration. For vehicles operating in a free-flowing traffic environment, Meng et al. [11] proposed a real-time online analytical speed planning method. This method was further extended to non-free-flowing traffic environments where other interfering vehicles exist, by incorporating optimal control strategies. Extensive simulations have demonstrated that this speed planning method meets requirements such as safety and energy-saving.

The aforementioned methods mainly focus on the energy-saving speed planning problem, while neglecting the longitudinal dynamic characteristics of vehicles and speed control issues, and mostly only consider speed planning for individual signal light section. Moreover, scholars have proposed a layered energy-saving speed planning and control method suitable for continuous signal lights road.

Considering the issues of energy-saving and collision avoidance, Liao et al. [12] proposed a layered speed planning and control system suitable for continuous signal lights road. In the upper layer, the system calculates the optimal reference speed to reduce energy consumption of EV. In the lower layer, the system combines the optimal reference speed and the collision avoidance objective function to compute the optimal acceleration of the system. Guo et al. [13] conducted research on Fuel Cell Hybrid Electric Vehicle (FCHEV). A dynamic programming algorithm is employed for speed planning. Model Predictive Controller (MPC) is used to solve the control input of the vehicle dynamics model. The proposed method can reduce hydrogen consumption while ensuring vehicle safety. Similarly, Yuan et al. [14] also adopted this method to reduce the energy consumption of FCHEV. Liu et al. [15] used a two-layer speed optimization and control method to solve the speed planning and energy management problems of FCHEV. The upper layer transforms the speed planning problem into a quadratic convex function, and uses the MOSEK solver to solve the function. The lower layer uses the alternating direction multiplier algorithm to obtain the input of the dynamics model. This method uses a lower computational cost to achieve the effect of reducing energy consumption.

Focusing on energy-saving, safety, and stable driving of vehicles, the aforementioned studies have carried out speed planning and control. However, the studies have neglected the impact of speed changes on ride comfort. Taking it a step further, Dong et al. [16] proposed an optimal speed control formula for EV on continuous signal lights road, considering energy consumption, traffic flow, battery life, and ride comfort. A* algorithm, iterative dynamic programming algorithm, and rearview speed optimization algorithm are utilized to solve the formula, thereby determining the optimal speed of EV. Similarly, Jin et al. [17] also adopted A* algorithm to solve the energy-saving problem of EV. Tang et al. [18] introduced a multi-objective layered optimization strategy, where the MPC-based speed planning strategy is utilized by upper level to achieve a balance between ride comfort and speed, while an energy management strategy based on adaptive equivalent consumption minimization is employed by the lower level to achieve the optimal power allocation.

After considering the existing research and theories on speed planning and control for continuous signal lights road, it is found that most of them are applicable to conventional fuel vehicles or hybrid vehicles. These studies primarily focus on the issues of longitudinal motion characteristics and energy-saving speed planning, while neglecting the issues of longitudinal dynamics characteristics and speed control. Moreover, the previous studies either focus on individual signal light intersection or have large acceleration magnitudes between multiple signal light sections, leading to ride discomfort.

Considering the energy consumption and ride comfort of EV on continuous signal lights road, the layered energy-saving speed planning and control method is proposed in this paper. The method includes the layer of energy-saving speed planning and the layer of MPC-based speed control. According to the states of the signal lights and the positions of EV, the energy-saving speed planning layer generates the energy-saving speed considering ride comfort. According to the longitudinal dynamics model of EV, the MPC-based speed control layer utilizes an MPC-based speed controller to generate torque commands, which allow EV to track the energy-saving speed. The novelties and contributions of this method are as follows.

(1) Most of the existing research primarily focuses on energy consumption of EV. This method extends and innovates on existing research by various methods, including reducing the number of stops of EV on continuous signal lights road, minimizing the range of speed change and adopting the sinusoidal variable speed curve to smooth acceleration process. It achieves the energy-saving speed considering ride comfort.
(2) Different from the existing research focusing on longitudinal motion characteristics and energy-saving speed planning, this method designs the MPC-based speed controller based on the longitudinal dynamics model and energy consumption model of

EV. The controller is simple in principle and easy to understand. It is also suitable for other research on EV and has certain application value.

(3) This method can reduce the energy consumption of EV, improve its range and ride comfort. This has important reference significance for promoting the development of EV and reducing the dependence of vehicles on fossil fuels.

The structure of the remaining parts of the paper is as follows: Section 2 introduces the principle of the utilized method. In section 3, the model of continuous signal lights road is established, and the method of energy-saving speed planning is described. In section 4, the longitudinal dynamics model of EV is established, and the MPC-based speed controller is designed. Section 5 illustrates the performance of the utilized method through simulation experiments. Section 6 emphasizes conclusions. The framework of this paper is shown in Fig. 1.

2. The principle of layered energy-saving speed planning and control method

The layered energy-saving speed planning and control method is aimed at reducing the energy consumption of EV and improving its ride comfort on continuous signal lights road. This method mainly includes an energy-saving speed planning layer and an MPC-based speed control layer. The principle is shown in Fig. 2.

As shown in Fig. 2: Based on information such as road traffic, signal lights, and EV position, the energy-saving speed planning layer calculates the feasible speed range for EV to pass through each signal light section without stopping. Furthermore, based on the principle of minimizing the range of speed change, the value in the speed range with the smallest difference from the initial speed of EV entering the section is selected as the energy-saving speed of this section. Taking it a step further, considering the impact of acceleration on ride comfort, a sinusoidal variable speed curve is employed to optimize the energy-saving speed for each section, ensuring a smooth acceleration process. The layer of energy-saving speed planning outputs energy-saving speeds considering ride comfort.

The MPC-based speed control layer utilizes the longitudinal dynamics model of EV to establish the MPC-based speed controller. Taking into account both speed tracking performance and energy consumption, the MPC-based speed controller outputs torque to control the speed of EV in accordance with the energy-saving speed. The layered planning and control method enables EV to pass through the continuous signal lights road without stopping, thereby reducing energy consumption and improving ride comfort.

3. Method of energy-saving speed planning

3.1. *Continuous signal lights road scene model*

This paper focuses on the research of energy-saving speed planning and control method for EV on continuous signal lights road. The structure and type of continuous signal lights road are not the main factors affecting the research. The following assumptions are made about the continuous signal lights road scene [19]:

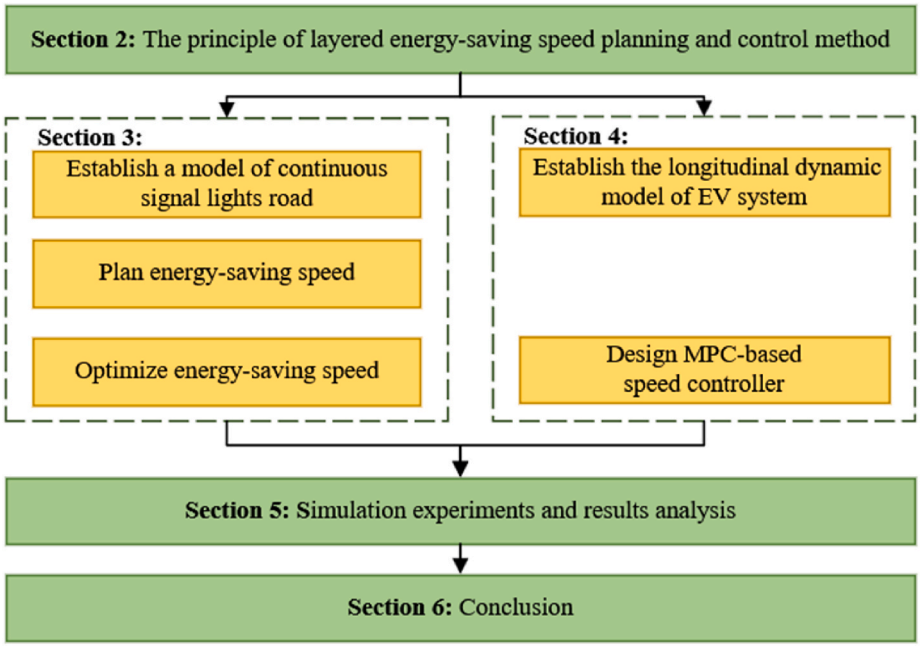

Fig. 1. The structure of the paper.

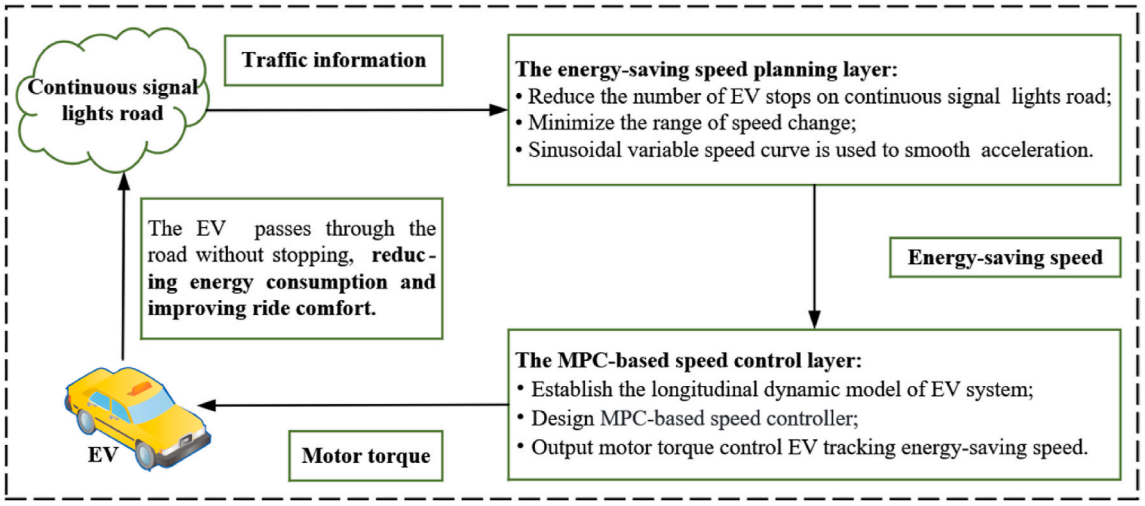

Fig. 2. The principle of layered energy-saving speed planning and control.

(1) The structure and type of signal light intersections are not considered, and the signal light intersections are simplified to stop lines;
(2) It is assumed that the continuous signal lights road is a one-way single-lane urban road, and the turning and lane changing situations of EV are not considered;
(3) It is assumed that all signal lights have only two phases, red and green. The duration of the yellow light is included in the duration of the red light, and all signal lights start from the red light phase. The initial phase offsets for all signal lights are set to zero;
(4) The speed limitations imposed on EV by factors such as traffic flow, weather conditions, etc., are uniformly considered as the road speed limits.

The completed continuous signal lights road model is shown in Fig. 3. In the model, T_{ri} represents the red light duration for the i-th signal light, T_{gi} represents the green light duration for the i-th signal light, and $T_{ci} = T_{gi} + T_{ri}$ represents the cycle duration for the i-th signal light, which includes both red and green light phases. $[V_{\min i}, V_{\max i}]$ represents the speed limit range for the i-th signal light section, which is determined by the traffic flow before and after EV and the speed limit of the road. S_i represents the distance from the EV to the i-th signal light, and $Dist_i = S_i - S_{i-1}$ represents the length of the i-th signal light section.

3.2. Energy-saving speed planning

The development of communication technologies such as Vehicle-to-Infrastructure (V2I), Vehicle-to-Vehicle (V2X), Sensors, and GPS have provided convenient conditions for EV to obtain signal light information and position. Assuming that the EV has obtained the

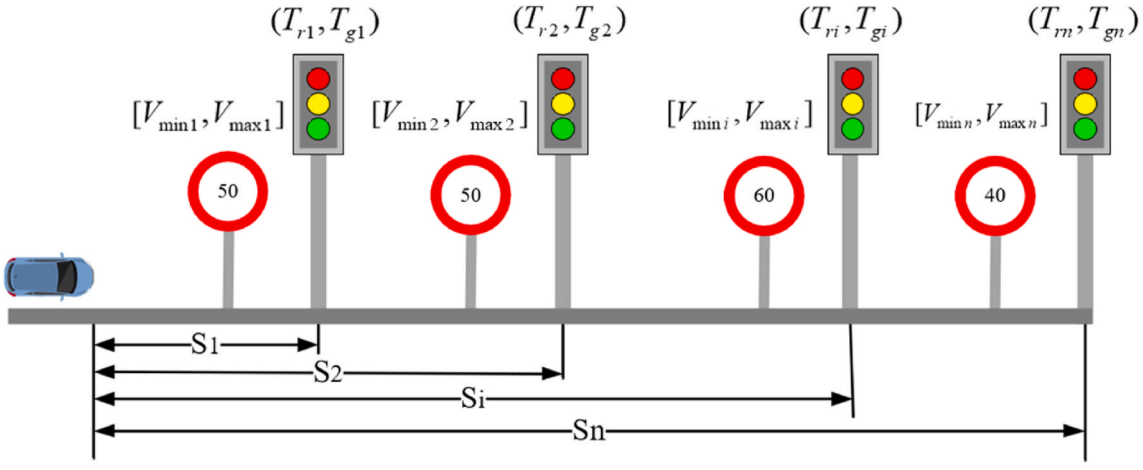

Fig. 3. Continuous signal lights road model.

following parameters of the i-th signal light section: $Dist_i$, S_i, T_{ci}, T_{ri}, T_{gi}, and $[V_{\min i}, V_{\max i}]$. The energy-saving speed planning for EV on continuous signal lights road is as follows:

Firstly, the time phase and signal phase of the i-th signal light at time t are calculated:

$$state_i = rem(t / T_{ci}) \tag{1}$$

$$f(state_i) = \begin{cases} 0 & 0 \le state_i \le T_{ri} \\ 1 & T_{ri} < state_i \le T_{gi} \end{cases} \tag{2}$$

In Eq. (1), t is the current time, that is, the total running time of EV; rem is the residual function; $state_i$ can represent the elapsed running time of the i-th signal light in a new cycle period at time t, that is, the time phase of the i-th signal light. In Eq. (2), $f(state_i)$ denotes the signal phase of the i-th signal light at time t. When $0 \le state_i \le T_{ri}$, $f(state_i) = 0$ indicates that the i-th signal light is in the red light phase; when $T_{ri} < state_i \le T_{gi}$, $f(state_i) = 1$ indicates that the i-th signal light is in the green phase.

Secondly, according to $f(state_i)$, S_i and $[V_{\min i}, V_{\max i}]$, the feasible speed range which makes EV pass through the i-th signal light section without stopping is calculated.

If the i-th signal light is in the red light phase at time t, the feasible speed range would be:

$$\begin{cases} V_{topi} = S_i / \left[state_i + T_{gi}(n-1) + T_{ri}(n-1)\right] \\ V_{lowi} = S_i / \left[state_i + T_{gi}n + T_{ri}(n-1)\right] \end{cases} \tag{3}$$

$$\begin{cases} n = n + 1 & [V_{\min i}, V_{\max i}] \cap [V_{lowi}, V_{topi}] = \varnothing \\ V_i \in [V_{lowi}, V_{\max i}] & (V_{\min i} \le V_{lowi}) and (V_{\max i} \le V_{topi}) \\ V_i \in [V_{lowi}, V_{topi}] & (V_{\min i} \le V_{lowi}) and (V_{\max i} \ge V_{topi}) \\ V_i \in [V_{\min i}, V_{topi}] & (V_{\min i} \ge V_{lowi}) and (V_{\max i} \ge V_{topi}) \end{cases} \tag{4}$$

In Eq. (3), n is an increasing positive integer with an initial value of 1. For each n, there is a corresponding $[V_{lowi}, V_{topi}]$. $[V_{lowi}, V_{topi}]$ represents the speed range at which the EV can pass through the i-th signal light intersection within its green light duration. In Eq. (4), V_i represents the feasible speed at which the EV can pass through the i-th signal light intersection without stopping. When $n = 1$, the corresponding $[V_{lowi}, V_{topi}]$ is intersected with the $[V_{\min i}, V_{\max i}]$. If the intersection exists, this intersection becomes the feasible speed range for EV to pass through the i-th signal light section without stopping. If the intersection does not exist, n is incremented by 1, and the process is repeated until an intersection exists.

If the i-th signal light is in the green light phase at time t, the feasible speed range would be:

$$V_{tempi} = S_i / (T_{ci} - state_i) \tag{5}$$

In Eq. (5), V_{tempi} represents the minimum speed at which EV can pass through the i-th signal light during the remaining green light time in the current cycle. If V_{tempi} satisfies $(V_{tempi} \le V_{\max i}) and (V_{tempi} \ge V_{\min i})$, the feasible speed range for EV to pass through the intersection without stopping is $[V_{tempi}, V_{\max i}]$. If V_{tempi} does not satisfies $(V_{tempi} \le V_{\max i}) and (V_{tempi} \ge V_{\min i})$, the feasible speed range can be researched in subsequent signal light cycles using Eqs. (6) and (4).

$$\begin{cases} V_{topi} = S_i / \left[T_{ci} - state_i + T_{gi}(n-1) + T_{ri}(n)\right] \\ V_{lowi} = S_i / \left[T_{ci} - state_i + T_{gi}n + T_{ri}(n)\right] \end{cases} \tag{6}$$

The meaning of the variable in Eq. (6) is the same as that in Eq. (3). Taking $n = 1, 2, 3\cdots\cdots$ in Eq. (6), there are corresponding $[V_{lowi}, V_{topi}]$, and bring the $[V_{lowi}, V_{topi}]$ into the Eq. (4) to obtain the feasible speed range. By sequentially iterating $i = 1, 2, 3, \ldots\ldots$, the feasible speed ranges for EV to pass through all sections of continuous signal lights road without stopping can be obtained.

Finally, based on the principle of minimizing the range of speed change, an energy-saving speed can be selected in the feasible speed range of each signal light section, so as to minimize the magnitude of speed changes on the continuous signal lights road. Suppose that the feasible speed range of the i-th signal light section is $[V_{lowi}, V_{\max i}]$, the principle for selecting the energy-saving speed for this road section is shown in Eq. (7):

$$\begin{cases} V_i = V_{\max i} & abs|V_{lowi} - V_x| \ge abs|V_{\max i} - V_x| \\ V_i = V_{lowi} & abs|V_{lowi} - V_x| \le abs|V_{\max i} - V_x| \end{cases} \tag{7}$$

In Eq. (7), V_x is the initial speed of EV entering the signal light section; V_i is the energy-saving speed of the i-th signal light section to be determined, and its value is the one in the range of $[V_{lowi}, V_{\max i}]$ with the smallest absolute difference from V_x. Furthermore, the method can be expressed as Fig. 4.

3.3. Energy-saving speed optimization

The signal lights divide the continuous road into different sections. Energy-saving speed planning can determine the energy-saving speed for EV to pass through each section without stopping. However, it may cause a step change in the speed at the junction of two sections, leading to unstable acceleration. This is detrimental to improving ride comfort and reducing energy consumption. Here, a sinusoidal variable speed curve is utilized to optimize the acceleration processes [20]. The function of sinusoidal variable speed curve is as follows:

$$V_{ai} = \begin{cases} V_i - V_d \cos(mt) & t \in [0, t_1) \\ V_i - V_j \cos\left[h\left(t - \frac{\pi}{2m} + \frac{\pi}{2h}\right)\right] & t \in [t_1, t_2) \\ V_i + V_j & t \in [t_2, T_i] \end{cases} \tag{8}$$

In Eq. (8), V_{ai} represents the sinusoidal variable speed curve. V_i is the energy-saving speed for EV to pass through the i-th signal light section without stopping. V_d represents the magnitude of speed change in the current signal light section, calculated as $V_d = V_i - V_x$, where V_x is the initial speed of EV entering this section. m, h, and V_j are parameters to be determined, which need to be adjusted based on V_d. $t_1 = \pi/2m$ and $t_2 = (\pi/2m) + (\pi/2h)$, where t_1 and $t_2 - t_1$ represent quarter cycle of $\cos(mt)$ and $\cos[h(t - \pi/2m + \pi/2h)]$ respectively. T_i represents the travel time for EV to pass through the current signal light section without stopping, and $T_i = Dist_i / V_i$. Taking positive acceleration as an example, the values of m, h, and V_j should make the optimized speed curve as shown in Fig. 5.

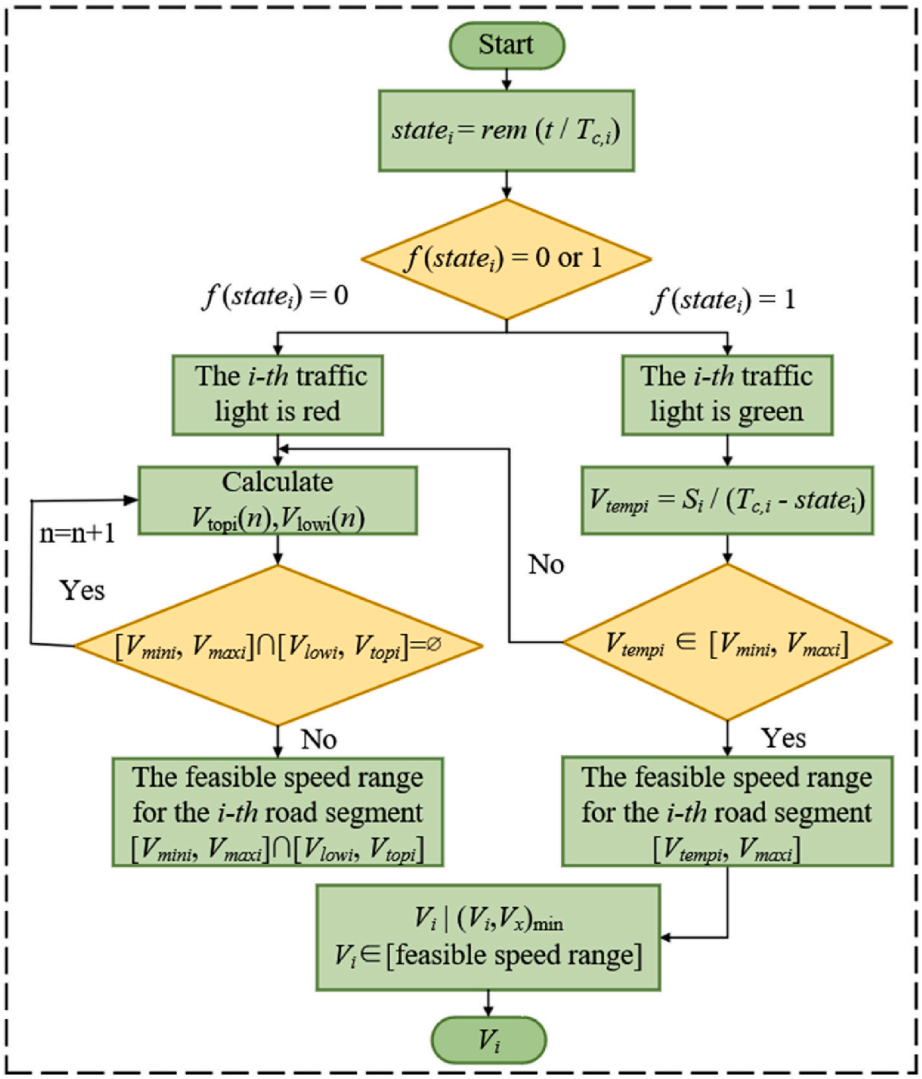

Fig. 4. Energy-saving speed planning.

According to Fig. 5, at the end of the first segment of the sinusoidal variable speed curve, the EV accelerates to V_i. At the end of the second segment of the sinusoidal variable speed curve, the EV accelerates to $V_j + V_i$ and maintains the speed for the remaining time. To ensure that EV can pass through the signal light intersection within green light time, the average speed of the signal light section should still be V_i, which requires that the integral of V_{ai} on $[0, T_i]$ is equal to the integral of V_i on $[0, T_i]$, that is, $S_1 = S_2$. Based on this, the rules for determining m, h, and V_j can be provided:

$$V_j = \begin{cases} \ln[abs(V_d) + 1\,] & V_i - V_d \geq 0 \\ -\ln[abs(V_d) + 1\,] & V_i - V_d < 0 \end{cases} \tag{9}$$

$$\int_0^{t_1} V_i - [V_i - V_d \cos(mt)]dt = \int_{t_1}^{t_1+t_2} V_i - V_j \cos[h(t - \pi/2m + \pi/2h)]dt + \int_{t_1+t_2}^{T_i} V_j dt \tag{10}$$

$$\begin{cases} (\pi/2m) + (\pi/2h) < T_i \\ h > 0 \\ m > 0 \end{cases} \tag{11}$$

Eq. (9) provides the rule for determining V_j, where the trend of V_j is consistent with V_d. Eqs. (10) and (11) represent the equality and inequality constraints that m, h, and V_j need to satisfy. Based on these constraints, Eq. (12) can be obtained:

$$\begin{cases} h = \left[mV_j(2 - \pi)\right] / \left(2V_d - 2mV_jT_i + V_j\pi\right) \\ \left[\left(2V_d + \pi V_j\right)/2V_jT_i\right] < m < \left[\left(\pi V_d + \pi V_j\right)/2V_jT_i\right] \end{cases} \tag{12}$$

Eq. (12) provides the relationship between h and m, and the range of m. As m increases, h also increases, resulting in smaller periods of the trigonometric functions and faster acceleration processes. Conversely, as m decreases, h decreases, resulting in larger periods of the trigonometric functions and smoother acceleration processes. Based on this observation, the trend of m should be opposite to the trend of V_d. The specific rule for determining m can be expressed as Eq. (13):

$$m = \left\{\left[2 + (\pi - 2)(\ln(abs(V_d) + 1) + 1)^{-1}\right]V_d + \pi V_j\right\} / 2V_jT_i \tag{13}$$

Eq. (13) ensures that the range of m satisfies Eq. (12), and as the magnitude of V_d increases, the acceleration processes become slower, conversely, as the magnitude of V_d decreases, the acceleration processes become faster. The optimized speed curve can adjust the acceleration time based on the magnitude of V_d, resulting in smooth acceleration processes, thereby improving ride comfort.

Additionally, the optimized speed curve satisfies the following conditions: when $t \in [0, t_1)$, the slope of the curve gradually increases, indicating an increasing acceleration; when $t \in [t_1, t_2)$, the slope of the curve gradually decreases, indicating a decreasing acceleration; when $t \in [t_2, T_i]$, the acceleration is zero. The process of gradually increasing acceleration and then decreasing it to zero is beneficial for improving ride comfort and reducing energy consumption.

3.4. The effect of energy-saving speed planning method

In this section, the speed obtained by the energy-saving speed planning method is compared with the normal speed. Consider the road scene with two continuous signal sections. The length of the first section is 600 m, the red light duration of the signal light is 20 s,

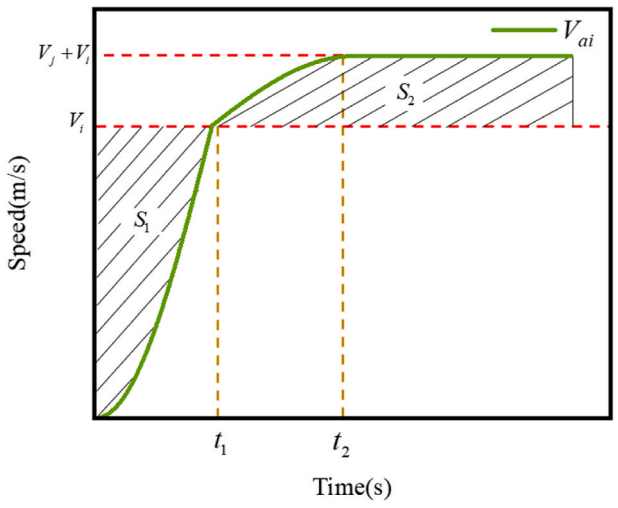

Fig. 5. The optimized speed curve.

and the green light duration is 10 s. The length of the second section is 500 m, the red light duration of the signal light is 15 s, and the green light duration is 15 s. The road speed limit is 15 m/s. The normal speed curve, the energy-saving speed curve and the optimized energy-saving speed curve for the road scene are shown in Fig. 6.

The orange curve in Fig. 6 represents the optimized energy-saving speed; the blue curve represents the energy-saving speed; the green curve represents the normal speed. It can be seen from the figure that when passing the road at normal speed, the passage time is 83 s, but there are speed leaps and emergency start-stop, which will cause additional energy consumption and ride discomfort. When passing the road at energy-saving speed, there is no problem of emergency start-stop, but there is still a problem of speed leaps and the passage time increases to 105 s. This is beneficial to reduce energy consumption, but it will cause ride discomfort. In contrast, the optimized energy-saving speed curve changes slowly and steadily. There is no speed leap and emergency start-stop, which is beneficial to reduce energy consumption and improve ride comfort. However, the travel time at this speed is increased to 105 s.

Therefore, compared with normal speed, the speed obtained by energy-saving speed planning method sacrifices less travel time, reduces energy consumption and improves ride comfort. In particular, this section clarifies qualitatively that the energy-saving speed planning method is beneficial to reducing energy consumption and improving ride comfort. Section 5 will analyze quantitatively the effect of the method on the reduction of energy consumption and the improvement of ride comfort.

4. Design of MPC-based speed controller

4.1. Longitudinal dynamic model of EV system

Since there is no lane changing or turning involved in the energy-saving speed planning, it is sufficient to establish the longitudinal dynamics model of EV system when controlling the speed of EV. Referring to Refs. [21,22], the model can be established by the control law or the input-output data sequence of the system. The longitudinal dynamics model of the EV system without braking force is as follows:

$$\begin{cases} \dot{s} = v \\ \dot{v} = (F_T/M\delta R) - \left(C_D\rho A v^2/2M\delta\right) - [Mgf\cos(\theta) + Mg\sin(\theta)]/M\delta \end{cases} \tag{14}$$

In Eq. (14), $\dot{s}$ and $\dot{v}$ are the differentials of the longitudinal position and velocity of the EV, and also the state variables of the EV system. F_T is the motor torque, and also the input of the EV system. M and R are the mass and wheel radius of the EV; δ is the concentrated rotational inertia coefficient; C_D is the air resistance coefficient; ρ is the nominal air density; A_s is the area of the front of the EV; g is the gravitational constant; θ is the inclination angle of the road, which can be set to 0 since the signal lights exist in the urban roads with less fluctuation; f is the rolling resistance coefficient, $f = 0.0122 \times (1 + v^2/19440)$. Consistent with reference [21], the values of other physical parameters are shown in Table 1.

Further, according to Eq. (14), the power equation at the wheels of EV and the output power of EV motor can be derived:

$$\begin{cases} p_m = \omega F_T \\ p_e = p_m \eta^k \end{cases} \tag{15}$$
$$if\ F_T < 0\ ,\ k = 1\ ;\ else\ k = -1$$

In Eq. (15), p_m represents the power at the wheels of EV; p_e represents the output power of EV motor; ω represents the rotational speed of wheels, and $\omega = v/R$; η represents the motor efficiency, whose value consistent with the value in Ref. [21]. The energy consumption model of EV system with regenerative braking is as follows:

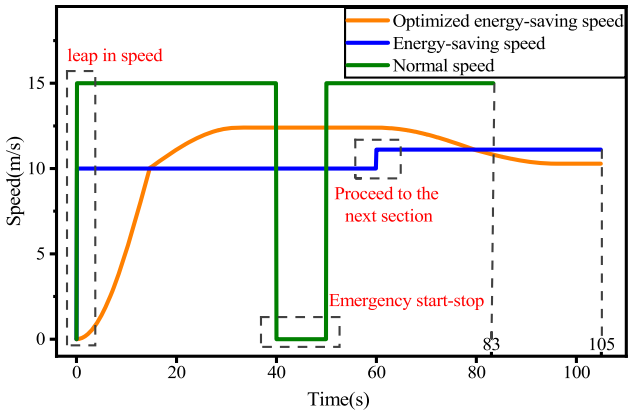

Fig. 6. Comparison of different speed curves.

Table 1
Parameters of longitudinal dynamic model of the EV system.

Symbol	Description	Value (Unit)
M	Vehicle mass	1874 (kg)
R	Wheel radius	0.33 (m)
δ	lumped rotational inertial coefficient	1
C_D	Drag coefficient	0.23
ρ	Air density	1.206 (kg/m^3)
A_s	Face area	2.6(m^2)
g	Gravitational constant	9.8(m/s^2)

$$E = \int_{t_0}^{t_n} p_e dt \tag{16}$$

In Eq. (16), E represents the energy consumption during EV driving process, with t_0 being the initial time and t_n being the final time.

For the convenience of calculation, the longitudinal dynamics model of the EV system presented at Eq. (14) can be transformed into a state-space form, as shown in Eq. (17):

$$\begin{cases} \dot{x} = Ax + Bu + g \\ y = x \end{cases} \tag{17}$$

In Eq. (17), $\dot{x}$ represents the derivative of the EV system state vector, and $\dot{x} = \begin{bmatrix} \dot{s} \\ \dot{v} \end{bmatrix}$; A and B are coefficient matrices, with $A = \begin{bmatrix} 0 & 1 \\ 0 & 0 \end{bmatrix}$ and $B = \begin{bmatrix} 0 \\ \frac{1}{MR} \end{bmatrix}$; x is the state vector of the EV system, and $x = \begin{bmatrix} s \\ v \end{bmatrix}$; u is the input of the EV system, and $u = F_T$; g_c is the system disturbance, and $g_c = \begin{bmatrix} 0 \\ -\frac{C_D \rho A v^2}{2M} - gf(v) \end{bmatrix}$.

4.2. MPC-based speed controller

By predicting the future behavior of the system, MPC optimizes the input of the system to achieve the best control effect. The basic principle of MPC is as follows [23]: Firstly, the system model is established: A mathematical model is established to describe the behavior of the system, which is completed in the first section of this chapter. Secondly, predict system behavior: The established model is used to predict the state and input of the system, so as to obtain the behavior of the system for a period of time in the future. Then optimize the input of the system: According to the predicted system behavior, the optimization algorithm is used to select the best input sequence of the system under a certain cost function. Finally, the system input is applied: the selected system input sequence is applied to change the system state. MPC can handle complex multivariable systems, and can cope with uncertainties and disturbances. Next, the MPC-based speed controller is designed by using the longitudinal dynamics model of the EV.

References [24,25] show that the method of discretizing differential equations and linearizing nonlinear equations is easy to understand and implement, and is widely accepted in the field of mathematics and physics. In order to facilitate the solution and control, Eq. (17) is discretized as sampling step $\triangle t$, and the discrete result is shown in Eq. (18):

$$\begin{cases} x(k+1) = A_c x(k) + B_c u_k + g_k \\ y(k+1) = x(k+1) \end{cases} \tag{18}$$

In Eq. (18), $A_c = I_2 + \triangle tA$, $B_c = \triangle tB$, and $g_k = \triangle t g_c$, where I_2 represents an identity matrix of order 2. Specifically, the variable v in matrix g_k is substituted with v_{ref}, where v_{ref} represents the reference speed, which is obtained from the output of the energy-saving speed planning layer. Replacing v with v_{ref} can linearize the system disturbance.

If the predicted time domain and the control time domain are both N, and the state of the EV system at time k is x_0, then the predicted input of the EV system at the $k+i$ moment is u_{i-1}, and the predicted state of the EV system at the $k+i$ moment is x_i,where $u_{i-1} = u(k+i-1|k)$ and $x_i = x(k+i|k)$. Combining with Eq. (18), the prediction equation is established as follows:

$$Y_k = X_k = Mx_0 + CU_k + G_k \tag{19}$$

In Eq. (19), Y_k represents the predicted output vector of the system for future N steps, and $Y_k = \begin{bmatrix} y_1 \\ y_2 \\ \cdots \\ y_N \end{bmatrix}$; X_k represents the predicted state

vector of the system for future N steps, and $X_k = \begin{bmatrix} x_1 \\ x_2 \\ \cdots \\ x_N \end{bmatrix}$, and according to Eq. (18), $Y_k = X_k$; U_k represents the predicted input vector of the system for future N steps, and $U_k = \begin{bmatrix} u_0 \\ u_1 \\ \cdots \\ u_{N-1} \end{bmatrix}$; M, C, and G_k are coefficient matrices expanded from A, B, and g_K respectively, and $M = \begin{bmatrix} A \\ A^2 \\ \cdots \\ A^N \end{bmatrix}$, $C = \begin{bmatrix} B & 0 & \cdots & 0 \\ AB & B & \cdots & 0 \\ \vdots & \vdots & \vdots & \vdots \\ A^{N-1}B & A^{N-2}B & \cdots & B \end{bmatrix}$, and $G_k = \begin{bmatrix} g_1 \\ Ag_1 + g_2 \\ \cdots \\ A^{N-1}g_1 + A^{N-2}g_2 + \cdots + g_N \end{bmatrix}$.

Considering the speed tracking error and energy consumption, the cost function is established as follows:

$$J = \left(X_k - X_{ref}\right)^T Q \left(X_k - X_{ref}\right) + U^T R U \tag{20}$$

In Eq. (20), J is the cost function; X_{ref} is the reference state vector within the prediction time domain, including the driving speed output from the energy-saving speed planning layer and the corresponding driving distance based on the speed; Q is the state weight matrix, with $Q = I \otimes q$, where I is the unit matrix of $N \times 2$ order, $q = \begin{bmatrix} q_s & \\ & q_v \end{bmatrix}$, and q_s, q_v are the weights of driving distance and driving speed respectively; R is the input weight matrix, and $R = I \otimes q_{F_T}$, where q_{F_T} is the weight of input torque. The values of q_s, q_v and q_{F_T} affect the tracking effect of the speed controller on the energy-saving speed and can be obtained by adjusting the MPC toolbox in MATLAB. The motor torque and speed constraints are as follows:

$$\begin{cases} \min(F_T) \le u \le \max(F_T) \\ V_{\min} \le v \le V_{\max} \\ S_0 \le s \le S_n \end{cases} \tag{21}$$

Eq. (21) specifies the upper and lower limits of motor torque F_T, system state v and s.

The MPC-based controller transforms the speed control problem into a cost function solution problem with constraints. Reference [26] shows that by transforming the problem to be solved into function analysis, a more accurate calculation result can be obtained with a smaller amount of calculation. Furthermore, by taking Eq. (19) into Eq. (20), the problem can be transformed into a constrained quadratic programming problem, which can be solved by using the quadprog function in MATLAB. The result is as follows:

$$J = 0.5U^T \left(C^T Q C + R\right) U + \left(\left(M x_0 + G_k\right)^T Q C - {X_{ref}}^T Q C\right) U \tag{22}$$

The input vector U of the EV system is obtained by solving Eqs. (21) and (22) with the quadprog function, and the first element of U is applied to the system.

5. Simulation verification

5.1. Description of the simulation scene

Based on the Matlab/Simulink platform, a model of energy-saving speed planning and control is built and simulated. The simulation scenario is a road with four continuous signal lights. The minimum speed on the road is set to 0 m/s, and the maximum speeds are set to 10 m/s, 15 m/s and 20 m/s respectively. The initial speed of the EV is 0 m/s, and the phase and position information of the signal lights are shown in Table 2.

Table 2
The phase and position information of the signal lights.

The position of the traffic light S_i (m)	The time of red traffic light T_{ri} (s)	The time of green traffic light T_{gi} (s)
600	20	10
1100	15	15
1700	10	20
2100	15	10

5.2. Simulation verification

Signal lights are commonly found on urban roads. According to the data from Ref. [27], the speed limit on urban expressways is 60∼80 km/h, the speed limit on main roads and secondary roads is 50 km/h, and the speed limit on residential area roads is 20∼30 km/h. Therefore, in this part, the maximum speeds on the road are set to 10 m/s, 15 m/s and 20 m/s respectively. The simulation is performed with $V_{\max} = 20m/s$, and the simulation results are shown in Fig. 7.

The Fig. 7(a) represents the time of EV passing through each signal light intersection, where the green lines indicate the duration of the green light phase of the corresponding signal light; the red lines indicate the duration of the red light phase of the corresponding signal light, the blue dotted line indicates the driving distance of the EV when running in accordance with the reference speed strictly, where the reference speed is the speed produced by the energy-saving speed planning layer; and the brown dotted line indicates the actual driving distance of EV under control of the speed controller, also indicating the tracking effect of EV on the reference driving distance.

The Fig. 7(b) represents the torque and speed of EV, where the blue line indicates the speed produced by the energy-saving speed planning layer; the orange line indicates the actual speed of EV under the control of the speed controller, indicating the tracking effect of EV on the reference speed; and the dark green dotted line indicates the output torque of the speed controller, which controls EV to track the speed produced by the energy-saving speed planning layer.

Based on Fig. 7, it can be concluded that when $V_{\max} = 20m/s$: (1) The EV can pass through continuous signal lights road without stopping, and the passing time is mostly at the beginning or end of the green light phase. It is important to note that in the simplified model of the continuous signal light intersections, the intersection is represented by a stop line, and the duration of the yellow light is included within the duration of red light. Therefore, it is reasonable for EV to pass through the intersection when the green light phase is about to end. (2) The torque output from the speed controller effectively controls EV to track the speed and travel distance given by the energy-saving speed planning layer. (3) The maximum variation in speed occurs during the initial acceleration of EV. Afterward, the speed variation remains within 5 m/s, and the acceleration processes are smooth. (4) Based on the above three points, the method can enable EV to pass through continuous signal lights road without stopping, reducing energy consumption and maintaining ride comfort.

The simulation results of $V_{\max} = 15m/s$ and $V_{\max} = 10m/s$ are shown in Fig. 8.

The meaning of the lines in Fig. 8(a) and (c) is consistent with Fig. 7(a), and the meaning of the lines in Fig. 8(b) and (d) is consistent with Fig. 7(b). Furthermore, the conclusions drawn from Fig. 8 are consistent with those from Fig. 7. The proposed layered energy-saving speed planning and control method allows the EV to pass through continuous signal lights road without stopping, reducing energy consumption and improving ride comfort.

5.3. Analysis of simulation results

This section discusses and analyzes the performance of the utilized method based on simulation data. The performance of this method is mainly reflected in the following three aspects: the appropriateness of MPC-based speed controller, the energy consumption level and ride comfort of EV.

The method of goodness-of-fit test can verify the fitting degree between the actual speed curves of EV and the reference speed curves under different $V_{\max}$ values, so as to illustrate the appropriateness of MPC-based speed controller. The value of *R-squared* is calculated by the method to compare the fitting degree of two curves. The value of *R-squared* is between 0 and 1, and the closer to 1, the better the fitting degree. The value of *R-squared* is calculated by Eq. (23):

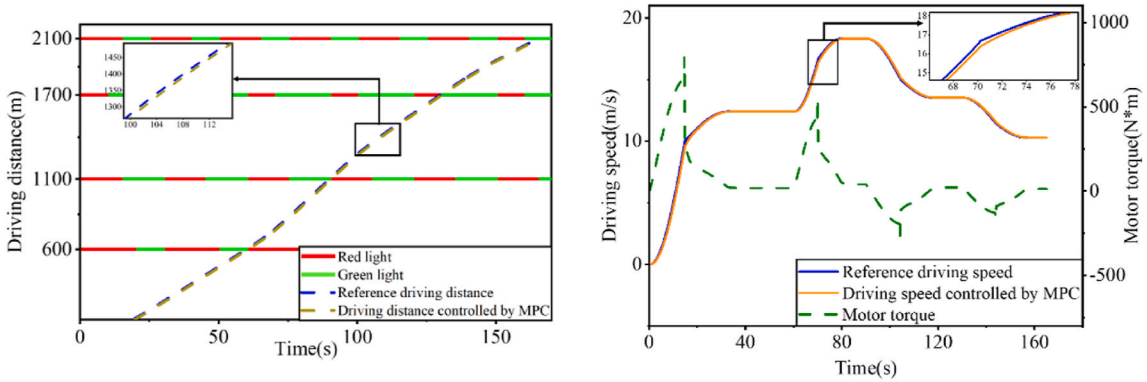

(a) The time of EV passing through each signal light intersections.

(b) The torque and travel speed of the EV.

Fig. 7. Simulation results of $V_{\max} = 20$ m/s.

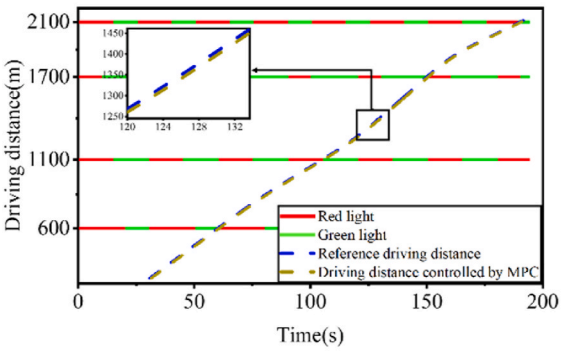

(a) The time of EV passing through each signal light intersection (V_{max}=15m/s).

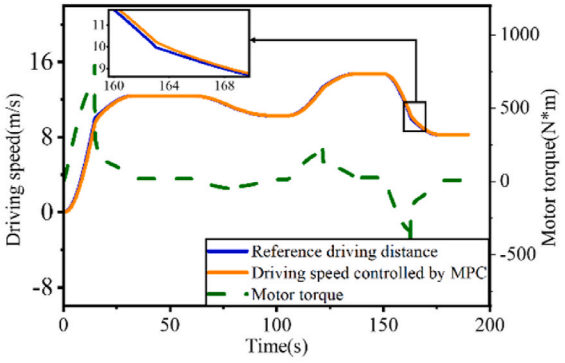

(b) The torque and travel speed of the EV (V_{max}=15m/s).

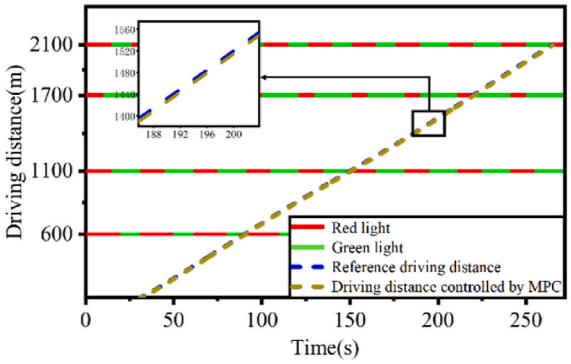

(c) The time of EV passing through each signal light intersection (V_{max}=10m/s).

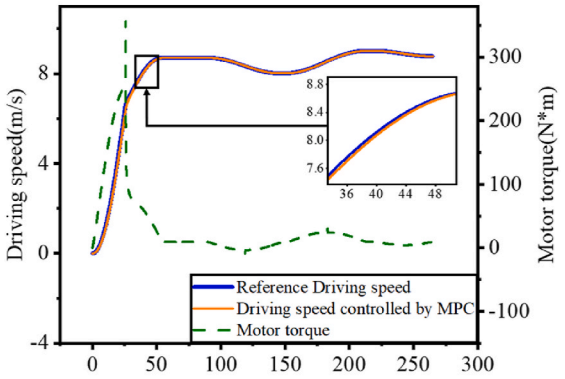

(d) The torque and travel speed of the EV (V_{max}=10m/s).

Fig. 8. Simulation results of V_{max} = 15 m/s and V_{max} = 10 m/s.

$$\begin{cases} SSE = sum\left(\left(v_{act} - v_{ref}\right)^2\right) \\ SST = sum\left(\left(v_{act} - mean\left(v_{act}\right)\right)^2\right) \\ R - squared = 1 - SSE/SST \end{cases} \tag{23}$$

In Eq. (23), v_{act} represents the actual speed curve; v_{ref} represents the reference speed curve; *sum* represents the function of summation; *mean* represents the function of mean; *SSE* represents the sum of squared residuals; *SST* represents the total sum of squares. Under different V_{max} values, the *R-squared* values of the actual speed curves and the reference speed curves are shown in Table 3.

It can be seen from Table 3 that the values of *R-squared* are very close to 1, that is, the fitting degree between the actual speed curves of EV and the reference speed curves is very high, which means the MPC-based speed controller can control EV to run strictly in accordance with the reference speed, and the controller is very appropriate.

In order to better illustrate the utilized method can reduce the energy consumption of the EV driving on the continuous signal lights road, the energy consumption of EV (E) is calculated by Eqs. (15) and (16) when $V_{max} = 20m/s$, $V_{max} = 15m/s$ and $V_{max} = 10m/\ s$.

The standards [28,29] stipulate that the Root Mean Square (*RMS*) of weighted accelerations is used to evaluate ride comfort. The calculation method of the *RMS* of weighted accelerations is as follows: According to the different vibration frequencies felt by the

Table 3
The calculation results of *R-squared* under different V_{max} values.

V_{max} *R-squared*	$V_{max} = 10m/s$	$V_{max} = 15m/s$	$V_{max} = 20m/s$
R-squared	0.9996	0.9988	0.9991

Table 4
The calculation results of E and RMS_a under different V_{max} values.

E/RMS_a	$V_{max} = 20m/s$	$V_{max} = 15m/s$	$V_{max} = 10m/s$
E (kJ)	1269	785	514
E/km (kJ/km)	604.29	373.81	244.76
RMS_a (m/s^2)	0.25	0.13	0.10

human body in the acceleration time history, the accelerations at different times are assigned weights respectively, and the *RMS* of the accelerations is calculated on this basis. However, due to the assumption that the slope of the road surface is 0 and does not change, the acceleration weights can be kept constant and both are 1, and the *RMS* of weighted accelerations is equivalent to the *RMS* of accelerations. The acceleration value of EV at each sampling point and the *RMS* of the values can be calculated by Eqs. (14) and (24) respectively.

$$RMS_a = \sqrt{1 \Big/ dot\left(\sum_{i=1}^{dot}(a_i^2)\right)} \tag{24}$$

In Eq. (24), RMS_a represents the *RMS* of acceleration values, *dot* represents the total number of sampling points, and a_i represents the acceleration value at each sampling point.

When $V_{max} = 20m/s$, $V_{max} = 15m/s$, and $V_{max} = 10m/s$, the calculation results of E and RMS_a are shown in Table 4.

Based on Tables 4 and it can be observed that when $V_{max} = 20m/s$, the energy consumption of the EV is 604.29 kJ/km; when $V_{max} = 15m/s$, the energy consumption is 373.81 kJ/km, and when $V_{max} = 10m/s$, it is 244.76 kJ/km. Since the parameters of EV model and simulation scene in this paper are similar to those in literature [12], the energy consumption of EV obtained in the two papers is comparable. When $V_{max} = 20m/s$, the energy consumption obtained in Reference [12] is 786.60 kJ/km, and the energy consumption obtained in this paper is 604.29 kJ/km. In contrast, the method proposed in this paper can save 23.18 % of energy consumption. More general, under various driving conditions, including stop-and-go, free-flowing, and high-speed driving, the United States Environmental Protection Agency conducted energy consumption tests on multiple models of family EVs with an average speed range of 9.46–21.62 m/s. The test results showed that the energy consumption of the top 10 EVs ranged from 537.00 to 827.46 kJ/km [30]. Considering the simulation conditions are simplified and idealized of real-world conditions, it can be concluded that when $V_{max} = 20m/s$, the energy consumption of EV is within the average range and at a relatively low level; when $V_{max} = 15m/s$ and $V_{max} = 10m/s$, the energy consumption of EV is lower than the lowest level observed in actual road tests. Therefore, it can be inferred that the layered energy-saving speed planning and control method can make the energy consumption of EV at a low level.

Based on Table 4, when $V_{max} = 20m/s$, $RMS_a = 0.25$ m/s^2; when $V_{max} = 15m/s$, $RMS_a = 0.13$ m/s^2; and when $V_{max} = 10m/s$, $RMS_a = 0.10$ m/s^2. According to the standards [28,29], when RMS_a is 0.1 m/s^2 or below, the ride comfort of EV is better; When RMS_a is within the range of 0.1–0.315 m/s^2, the ride comfort of EV is general, and there is no uncomfortable phenomenon; and when RMS_a exceeds 0.315 m/s^2, the ride comfort of EV noticeably decreases. Therefore, when $V_{max} = 20m/s$, the ride comfort of EV is general, and there is no uncomfortable situation for passengers; when $V_{max} = 10m/s$ and $V_{max} = 15m/s$, the EV provides better ride comfort. The layered energy-saving speed planning and control method can make EV maintain better ride comfort.

Further, according to the above discussions and analyses, the following conclusions can be drawn.

(1) Under different V_{max} values, the *R-squared* values of the actual speed curves and the reference speed curves are all above 0.99, which indicates that the fitting degree of the two speed curves is high, further indicating the appropriateness of MPC-based speed controller.
(2) When the values of V_{max} are 20 m/s, 15 m/s and 10 m/s, the values of EV energy consumption are 604.29 kJ/km, 373.81 kJ/km and 244.76 kJ/km, respectively. The energy consumption is lower than that of actual road test, and can be saved by 23.18 % compared with the method proposed in the literature review, which means that the utilized method can reduce energy consumption of EV.
(3) When the values of V_{max} are 20 m/s, 15 m/s and 10 m/s, the values of RMS_a are 0.25 m/s^2, 0.13 m/s^2 and 0.10 m/s^2, respectively. When the value of RMS_a is less than 0.315 m/s^2, the ride comfort is better. The utilized method can make EV maintain good ride comfort.

6. Conclusion

To address the issues of increased energy consumption and decreased ride comfort caused by frequent start-stop during EV driving on continuous signal lights road, the layered energy-saving speed planning and control method is proposed.

(1) Energy-saving speed planning layer: By reducing the number of stops of EV on continuous signal lights road, minimizing the range of speed change and optimizing the acceleration process with sinusoidal variable speed curve, the energy-saving speed considering ride comfort is obtained.

(2) MPC-based speed control layer: The MPC-based speed controller is designed based on the longitudinal dynamics model and energy consumption model of EV. The controller transforms the speed control problem into a constrained quadratic programming problem to control EV driving. It is also suitable for other research on EV and has certain application value.
(3) A layered energy-saving speed planning and control model is built and simulated on the MATLAB/Simulink platform. The simulation results show that the utilized method can reduce energy consumption of EV and improve its ride comfort. This has important reference significance for promoting the development of EV.

The disadvantage of the utilized method is to consider the speed limitations imposed by the preceding and following traffic flow as road speed limits, and does not study the longitudinal collision avoidance method, which is the direction of further research.

Funding statement

This work was supported by the National Natural Science Foundation of China, China [grant number 52372357]; the Key Research and Development Program of Jiangsu Province, China [grant number BE2022146]; the Open Fund for State Key Laboratory of Automotive Simulation and Control, China [grant number 20210205]; and the Research Foundation of Nanjing Institute of Technology, China [grant number. CKJA202205].

Data availability statement

No data was used for the research described in the article.

Additional information

No additional information is available for this paper.

CRediT authorship contribution statement

Jing Jiao: Methodology, Formal analysis, Conceptualization. **Liguo Zang:** Supervision, Project administration, Funding acquisition. **Yulin Mao:** Software, Investigation, Data curation. **Cheng Xue:** Validation, Investigation. **Xinlei Peng:** Writing – review & editing, Writing – original draft.

Declaration of competing interest

The authors declare that they have no known competing financial interests or personal relationships that could have appeared to influence the work reported in this paper.

References

[1] Y. Shen, Y. Li, C. Chen, J. Li, Electric vehicle scheduling based on stochastic trip time and energy consumption, Comput. Ind. Eng. 177 (2023), 109071, https://doi.org/10.1016/j.cie.2023.109071.
[2] C. Sun, B. Liu, F. Sun, Review of energy-saving planning and control technology for new energy vehicles, J. Automot Saf. Energy Sav. 13 (4) (2022) 593–616, https://doi.org/10.3969/j.issn.1674-8484.2022.04.001.
[3] K. Jin, X. Li, W. Wang, X. Hua, W. Long, Energy-optimal speed control for connected electric buses considering passenger load, J. Clean. Prod. 385 (2023), 135773, https://doi.org/10.1016/j.jclepro.2022.135773.
[4] L. Wu, Research based on the application of automobile new energy and energy-saving technology, Auto Time. 16 (2021) 111–113, https://doi.org/10.3969/j.issn.1672-9668.2021.16.053.
[5] J. Leng, C. Sun, B. Lu, Fast energy saving speed planning through multi signal intersections of intelligent vehicles, Automat. Eng. 43 (10) (2021) 1442–1447+1478, https://doi.org/10.19562/j.chinasae.qcgc.2021.10.004.
[6] J. Han, D. Shen, D. Karbowski, A. Rousseau, Leveraging multiple connected traffic light signals in an energy-efficient speed planner, IEEE Contr. Syst. Lett. 5 (6) (2021) 2078–2083, https://doi.org/10.1109/LCSYS.2020.3047605.
[7] H. Chen, W. Zhuang, G. Yin, H. Dong, Eco-driving control strategy of connected electric vehicle at signalized intersection, J. SEU (Nat. Sci. Edit.). 51 (1) (2021) 178–186, https://doi.org/10.3969/j.issn.1001-0505.2021.01.024.
[8] W. Zhuang, H. Ding, H. Dong, G. Yin, Q. Wang, C. Zhou, L. Xu, Learning based eco-driving strategy of connected electric vehicle at signalized intersection, J. JLU (Eng. Technol. Edit.). 53 (1) (2023) 82–93, https://doi.org/10.13229/j.cnki.jdxbgxb20210598.
[9] W. Wu, L. Huang, R. Du, Simultaneous optimization of vehicle arrival time and signal timings within a connected vehicle environment, Sensors. 20 (1) (2020), 191, https://doi.org/10.3390/s20010191.
[10] Z. Nie, H. Farzaneh, Real-time dynamic predictive cruise control for enhancing eco-driving of electric vehicles, considering traffic constraints and signal phase and timing (SPaT) information, using artificial-neural-network-based energy consumption model, Energy. 241 (2022), 122888, https://doi.org/10.1016/j.energy.2021.122888.
[11] X. Meng, C.G. Cassandras, Eco-Driving of autonomous vehicles for nonstop crossing of signalized intersections, IEEE Trans. Autom. Sci. Eng. 19 (1) (2022) 320–331, https://doi.org/10.1109/TASE.2020.3029452.
[12] G. Liao, L. Zheng, Z. Zhang, Y. Li, Y. Yu, Optimal speed planning and collision avoidance control for electric vehicles considering traffic lights, Sci. Sin. Technol. 52 (7) (2022) 1134–1144, https://doi.org/10.1360/SST-2021-0133.
[13] J. Guo, H. He, J. Li, Q. Liu, Real-time energy management of fuel cell hybrid electric buses: fuel cell engines friendly intersection speed planning, Energy. 226 (2021), 120440, https://doi.org/10.1016/j.energy.2021.120440.
[14] J. Yuan, J. Shao, W. Han, B. Wang, Hierarchical energy saving optimization control of intelligent networked hybrid electric vehicle, J. SDUT (Nat. Sci. Edit.). 37 (3) (2023) 54–61, https://doi.org/10.3969/j.issn.1672-6197.2023.03.011.

[15] B. Liu, C. Sun, B. Wang, W. Liang, Q. Ren, J. Li, F. Sun, Bi-level convex optimization of eco-driving for connected Fuel Cell Hybrid Electric Vehicles through signalized intersections, Energy. 252 (2022), 123956, https://doi.org/10.1016/j.energy.2022.123956.
[16] H. Dong, W. Zhuang, B. Chen, Y. Lu, S. Liu, L. Xu, D. Pi, G. Yin, Predictive energy-efficient driving strategy design of connected electric vehicle among multiple signalized intersections, Transport Res. C.-Emer. 137 (2022), 103595, https://doi.org/10.1016/j.trc.2022.103595.
[17] H. Jin, R. Niu, Economic speed planning based on A-Star algorithm for intelligent vehicle in traffic light intersection, J. BIT. 43 (6) (2023) 595–601, https://doi.org/10.15918/j.tbit1001-0645.2022.165.
[18] X. Tang, Z. Duan, X. Hu, H. Pu, D. Cao, X. Lin, Improving ride comfort and fuel economy of connected hybrid electric vehicles based on traffic signals and real road information, IEEE Trans. Veh. Technol. 70 (4) (2021) 3101–3112, https://doi.org/10.1109/TVT.2021.3063020.
[19] W. Liu, Research on Economic Speed Planning Method for Electric Vehicles on Urban Roads, Tsinghua University, Beijing, 2021, https://doi.org/10.27266/d.cnki.gqhau.2021.000049.
[20] H. Xia, Eco-Approach and Departure Techniques for Connected Vehicles at Signalized Traffic Intersections, 2014. Retrieved from, https://www.proquest.com/dissertations-theses/eco-approach-departure-techniques-connected/docview/1564215335/se-2.
[21] J. Wang, J. Tong, Z. Qian, J. Yang, J. Liu, C. Dai, H. Sun, S. Li, Robust Predictive Energy-Saving Cruise Control of a Four-Wheel Electric Vehicle with an Air Conditioning System via a Generalized Proportional Integral Observer, 2022 6th CAA International Conference on Vehicular Control and Intelligence (CVCI), Nanjing, China, 2022, pp. 1–8, https://doi.org/10.1109/CVCI56766.2022.9964674.
[22] Z. Abo-Hammour, O. Alsmadi, S. Momani, O. Abu Arqub, A genetic algorithm approach for prediction of linear dynamical systems, Math. Probl. Eng. 2013 (2013), 831657, https://doi.org/10.1155/2013/831657.
[23] A. Altan, R. Hacıoğlu, Model predictive control of three-axis gimbal system mounted on UAV for real-time target tracking under external disturbances, Mech. Syst. Signal Process. 138 (2022), 106548, https://doi.org/10.1016/j.ymssp.2019.106548.
[24] Z. Abo-Hammour, O. Abu Arqub, S. Momani, N. Shawagfeh, Optimization solution of Troesch's and Bratu's problems of ordinary type using novel continuous genetic algorithm, Discrete Dynam. Nat. Soc. 2014 (2014), 401696, https://doi.org/10.1155/2014/401696.
[25] D. Patricia, V. Josué, A study of a meromorphic perturbation of the sine family, Demonstr. Math. 55 (1) (2022) 963–977, https://doi.org/10.1515/dema-2022-0183.
[26] O. Abu Arqub, Z. Abo-Hammour, Numerical solution of systems of second-order boundary value problems using continuous genetic algorithm, Inf. Sci. 279 (2014) 396–415, https://doi.org/10.1016/j.ins.2014.03.128.
[27] National Bureau of Statistics, China Statistical Yearbook, 2023. http://statsdatabank.com/. (Accessed 7 July 2023).
[28] ISO 2631-1: 1997(E), Mechanical Vibration and Shock - Evaluation of Human Exposure to Whole-Body Vibration - Part 1: General Requirements, International Organization for Standardization, 1997.
[29] GB/T 4970-2009, Test Method for Automotive Smoothness: General Requirements, China Standards Publishing House, Beijing, 2009.
[30] U.S. Environmental Protection Agency and U.S.. Department of Energy. "Find a Car"., Fuel Economy, 2023. https://www.fueleconomy.gov/feg/findacar.shtml. 2023. (Accessed 7 July 2023).